AIMS Mathematics, 11(1): 420–443.
DOI:10.3934/math.2026018
Received: 12 November 2025
Revised: 15 December 2025
Accepted: 29 December 2025
Published: 06 January 2026

https://www.aimspress.com/journal/Math

Research article

New solitary wave solutions for the triplet coupled nonlinear Schrödinger system incorporating fractional effects

Tahani A. Alrebdi[1], Nauman Raza[2,3], Saima Arshed[2], F. Alkallas[1] and Abdel-Haleem Abdel-Aty[4,5,*]

[1] Department of Physics, College of Science, Princess Nourah bint Abdulrahman University, P.O. Box 84428, Riyadh 11671, Saudi Arabia
[2] Institute of Mathematics, University of the Punjab, Lahore 54590, Pakistan
[3] Research Center of Astrophysics and Cosmology, Khazar University, Baku, AZ1096, 41 Mehseti Street, Azerbaijan
[4] Department of Physics, College of Sciences, University of Bisha, Bisha 61922, Saudi Arabia
[5] Physics Department, Faculty of Science, Al-Azhar University, Assiut 71524, Egypt

* **Correspondence:** Email: amabdelaty@ub.edu.sa.

Abstract: New traveling wave solutions for the nonlinear fractional Schrödinger equation (FSE), obtained using conformable fractional derivatives, are presented in this paper. Despite extensive research on classical and fractional Schrödinger models, a systematic development of accurate traveling wave solutions employing conformable operators in conjunction with effective symbolic approaches remains lacking. To bridge this gap, we employ a Hamiltonian-based technique, a variational formulation via the Ritz method, and the modified Sardar subequation method. The fractional governing model is reduced to a nonlinear ordinary differential equation through a complex traveling wave transformation, which is analytically solved to yield new families of solutions. Two- and three-dimensional graphical representations of the solution's physical properties are presented, emphasizing the wave dynamics of the proposed fractional model.

Keywords: fractional Schrödinger equations; variational principle; variational method; Hamiltonian-based method
Mathematics Subject Classification: 35C08, 35R11, 37K40

1. Introduction

Fractional partial differential equations (FPDEs) are effective tools for simulating nonlinear systems in disciplines such as electromagnetics, geophysics, fluid mechanics, and economics [1,2]. As a result,

they have attracted considerable attention in the mathematical and physical sciences. The theory of fractional calculus provides a wide variety of fractional operators, which are employed to comprehend and modeling a wide range of biological and physical phenomena [3–5]. These operators enable more precise representations of complex systems, particularly those exhibiting memory and hereditary characteristics [6, 7].

The nonlinear Schrödinger equation (NFSE), regarded as one of the most reliable quantum models, quantum mechanical phenomena. This model encompasses a wide range of state wave functions in nonlinear media, including damping, diffusion, heat transport, and plasmas. Feynman and Hibbs employed path integrals over Brownian trajectories to establish the classical Schrödinger equations for the first time in 1965. Fractional-order Schrödinger equations were subsequently formulated by replacing Brownian trajectories with Levy trajectories [8]. Laskin later modified the space-time fractional Schrödinger equation to incorporate the quantum Riesz fractional framework [9]. Since then, NFSEs have attracted significant attention within the scientific community [10]. For example, Naber (2004) employed Caputo fractional derivatives to evaluate the time-dependent NFSE [11], while Guo et al. (2008) applied energy methods [12] to study the existence and uniqueness of solutions. In [13], asymptotic analysis of double-hump solitons was conducted for a coupled fourth-order nonlinear Schrödingier system in a birefringent optical fiber. Eid et al. (2009) addressed the space-dependent NFSE using the Coulomb potential [14], while Muslih et al. (2010) investigated the time-dependent FSEs and their solutions [15] via the Caputo technique. Furthermore, a new fractional operator based on the Mittag-Leffler function, a nonsingular kernel, and the Caputo-Fabrizio fractional derivative was introduced in (2017) as an alternative model for NFSEs [16]. Bakkyaraj and Sahadevan (2016) employed the homotopy analysis method [17] to obtain analytical and numerical solutions for coupled NFSEs. Overall, NFSEs provide a foundation for understanding Heisenberg dynamical model and for establishing connections between quantum and classical physics within the Lagrangian framework.

According to [8] and [9], the fractional Schrödinger equation was first used to characterize quantum systems with anomalous dispersion and nonlocal interactions. [18] and [19] have provided more evidence of its physical significance in nonlinear optics and wave propagation in complicated media. In parallel, multi-component wave interactions in Bose-Einstein condensates, plasma physics, and birefringent optical fibers have been extensively modeled using coupled nonlinear Schrödinger systems [20]. Fractional derivatives naturally extend classical models to incorporate memory and hereditary effects. The main motivation of the present study is to apply three efficient methods—the variational approach [21], the Hamiltonian-based method [22], and the Sardar subequation method [23] to construct precise analytical solutions for triple NFSEs [24].

$$\begin{aligned} D_{tx}^{\alpha\beta}u &= D_x^{\beta}(D_x^{\beta}(u)) + \frac{2|u|^2u}{1-h^2} + (v-w)u, \\ D_t^{\alpha}v &= -\frac{D_t^{\alpha}|u|^2}{h+1} + (1+h)D_x^{\beta}v, \\ D_t^{\alpha}w &= \frac{D_t^{\alpha}|u|^2}{1-h} + (1-h)D_x^{\beta}w. \end{aligned} \tag{1.1}$$

This model involves a complex-valued function $u(x,t)$ and real-valued functions $v = v(x,t)$ and $w = w(x,t)$, whereas h is a constant. Conformable fractional derivatives are defined for $0 < \alpha, \beta \leq 1$ with α and β denoting orders of fractional derivatives D_t^{α} and D_x^{β}, respectively.

By incorporating nonlocal and memory effects, fractional quantum-mechanics models generalize classical Schrödinger-type equations, as demonstrated in [24]. This enables for deeper soliton dynamics and provides precise solutions that are used as benchmarks for analytical and numerical investigations. Obtaining exact and accurate solutions for nonlinear fractional models is complex and intricate problem. In the recent, considerable efforts have been devoted to developing numerous numerical and analytical methods for solving nonlinear evolution equations, including the one Step Non-local Homotopy Perturbation Method [25], the Exp-function approach [26], the residual power series method [27], the unified method [28], the reproducing kernel method [29], the first integral method [30], Kudryashov method, the homogenous balance method [31], and the natural transform decomposition method [32]. The main aim of this research, is to construct new traveling wave solutions for the proposed fractional nonlinear model using the suggested techniques.

The structure of the present work is as follows: Section 2 introduces the basic definitions and notation of fractional calculus. Section 3 presents the semi-inverse method, while Section 4 discusses the Sardar subequation approach. Sections 5 and 6 apply these methods to compute traveling wave solutions of the triple nonlinear fractional Schrödinger equations. Section 7 provides visual representations of the obtained solutions are shown in Section 7. Exact observations and conclusions are presented in Section 8.

2. Conformable derivative

The Caputo definition, the Riemann-Liouville definition, the Atangana-Baleanu-Caputo definition, the Grunwald-Letnikov definition, and the conformable fractional derivative are some of the definitions of fractional operators that are frequently employed. The conformable fractional derivative is applied to the proposed model. The definition of the conformable derivative [33] of order is given as follows:

$$D_s^{\beta}(g(s)) = \lim_{\delta \to 0} \frac{g(\delta s^{1-\beta} + s) - g(s)}{\delta}, \ \beta \in (0, 1].$$

The conformable derivative possesses the following properties:
Property I: $D_{\xi}^{\beta} \xi^k = k\xi^(k - \beta)$,
Property II: $D_{\Lambda}^{\beta}(k_1\rho(\Lambda) \pm (k_2\eta(\Lambda)) = k_1 D_{\Lambda}^{\beta}(\rho(\Lambda)) \pm k_2 D_{\Lambda}^{\beta}(\eta(\Lambda))$,
Property III: $D_{\rho}^{\beta}\mu(\Lambda(\rho)) = \mu'_{\Lambda}(\Lambda(\rho)) D_{\rho}^{\beta}\Lambda(\rho)$.

In the present context, k, k_1, and k_2 represent real constants, while $\mu(\rho)$ and $\Lambda(\rho)$ are arbitrary differentiable functions.

3. Description of He's semi-inverse method

The aim of this section is to provide a summary of Heâs semi-inverse method. Let's look at the FPDE in the following form:

$$E(w, \partial_t^{\alpha} w, \partial_{\tau_1}^{\beta} w, \partial_{\tau_2}^{\gamma} w, ...) = 0, \quad 0 < \alpha, \beta, \gamma \leq 1, \tag{3.1}$$

where $w = w(t, \tau_1, \tau_2, \tau_3, ..., \tau_n)$. The following procedures are used to solve Eq (3.1).
First step: First, a variable transformation of the form is applied to Eq (3.1). $w(t, \tau_1, \tau_2, \tau_3, ..., \tau_n) = w(\Lambda)$, where Λ denotes a function of $t, \tau_1, \tau_2, \tau_3, ..., \tau_n$ and can be conveyed in a number of ways. This

transformation transforms Eq (3.1) into a nonlinear ordinary differential equation (NODE) with the following structure:

$$F(W, W', WW', ...) = 0. \tag{3.2}$$

The variable W in Eq (3.2) has derivatives about Λ. To find the constant(s) of integration, Eq (3.2) can occasionally be integrated once or more.

Second step: We create the following trial-functional using He's semi-inverse method:

$$J(W) = \int L d\Lambda = \int (K - E) d\Lambda, \tag{3.3}$$

where L is a function of W and its derivatives that is unknown. There are different methods for building the trial functionals.

Third step: Several types of single wave solutions can be obtained using the Ritz approach, including $U(\Lambda) = A\,\mathrm{sech}(B\Lambda)$, $U(\Lambda) = A\,\mathrm{csch}(B\Lambda)$, $U(\Lambda) = A\tanh(B\Lambda)$, $U(\Lambda) = A\coth(B\Lambda)$ and so on, where A and B are constants that need to be ascertained.

When the solitary wave solutions mentioned above are substituted into Eq (3.3) and J is made stationary with regard to A and B, the outcome is

$$\frac{\partial J}{\partial A} = 0, \tag{3.4}$$

$$\frac{\partial J}{\partial B} = 0. \tag{3.5}$$

We obtain A and B by simultaneously solving Eqs (3.4) and (3.5). The solitary wave solution is hence well defined.

4. Description of the Sardar sub-equation method

This section provides a detailed discussion of the suggested "SSEM" approach.

First step: Examine the structure below, which highlights the NLEE for

$$M(F, F_t, F_x, F_{xx}, F_{tt}, ...) = 0. \tag{4.1}$$

The traveling wave transformation $F(x, t) = h(\Lambda)$, where the wave variable Λ is defined as

$$\Lambda = \frac{k_1 x^{\beta}}{\Gamma(1+\beta)} + \frac{k_2 t^{\alpha}}{\Gamma(1+\alpha)} \tag{4.2}$$

is employed to transform Eq (4.1) into the subsequent ODE.

$$S(h, h', h'', h''', ...) = 0. \tag{4.3}$$

Second step: The following is the form of the solution to Eq (4.3):

$$h(\Lambda) = \sum_{i=0}^{N} q_i H^i(\Lambda). \tag{4.4}$$

In this case, the unknown constants to be solved are $q_i, (i = 0, 1, 2, 3, ..., N)$. Taking into account the auxiliary equation

$$H'(\Lambda) = \sqrt{c + \sigma H(\Lambda)^2 + gH(\Lambda)^4}, \tag{4.5}$$

here c, σ, and g are constants, and Eq (4.4) presents the solution as

Case 1: If $\sigma > 0$, and $c = 0$, then

$$H_1^{\pm}(\Lambda) = \pm\sqrt{-\frac{bp\sigma}{g}}\,\mathrm{sech}_{bp}(\sqrt{\sigma}\Lambda), \quad (g < 0),$$
$$H_2^{\pm}(\Lambda) = \pm\sqrt{\frac{bp\sigma}{g}}\,\mathrm{csch}_{bp}(\sqrt{\sigma}\Lambda), \quad (g > 0).$$

Case 2: If $\sigma < 0$, $g > 0$, and $c = 0$, then

$$H_3^{\pm}(\Lambda) = \pm\sqrt{-\frac{bp\sigma}{g}}\,\mathrm{sec}_{bp}(\sqrt{-\sigma}\Lambda),$$
$$H_4^{\pm}(\Lambda) = \pm\sqrt{-\frac{bp\sigma}{g}}\,\mathrm{csc}_{bp}(\sqrt{-\sigma}\Lambda).$$

Case 3: If $\sigma < 0$, $g > 0$, and $c = \frac{\sigma^2}{4g}$, then

$$H_5^{\pm}(\Lambda) = \sqrt{\frac{-\sigma}{2g}}\,\tanh_{bp}(\sqrt{\frac{-\sigma}{2}}\Lambda),$$
$$H_6^{\pm}(\Lambda) = \sqrt{\frac{-\sigma}{2g}}\,\coth_{bp}(\sqrt{\frac{-\sigma}{2}}\Lambda),$$
$$H_7^{\pm}(\Lambda) = \sqrt{\frac{-\sigma}{2g}}\left(\tanh_{bp}(\sqrt{-2\sigma}\Lambda) \pm \iota\sqrt{bp}\,\mathrm{sech}_{bp}(\sqrt{-2\sigma}\Lambda)\right),$$
$$H_8^{\pm}(\Lambda) = \sqrt{\frac{-\sigma}{2g}}\left(\coth_{bp}(\sqrt{-2\sigma}\Lambda) \pm \sqrt{bp}\,\mathrm{csch}_{bp}(\sqrt{-2\sigma}\Lambda)\right),$$
$$H_9^{\pm}(\Lambda) = \pm\sqrt{\frac{-\sigma}{8g}}\left(\tanh_{bp}(\sqrt{\frac{-\sigma}{8}}\Lambda) + \coth_{bp}(\sqrt{\frac{-\sigma}{8}}\Lambda)\right).$$

Case 4: If $\sigma > 0$, $g > 0$, and $c = \frac{\sigma^2}{4g}$, then

$$
\begin{aligned}
H_{10}^{\pm}(\Lambda) &= \sqrt{\frac{\sigma}{2g}}\tan_{bp}(\sqrt{\frac{\sigma}{2}}\Lambda),\\
H_{11}^{\pm}(\Lambda) &= \sqrt{\frac{\sigma}{2g}}\cot_{bp}(\sqrt{\frac{\sigma}{2}}\Lambda),\\
H_{12}^{\pm}(\Lambda) &= \sqrt{\frac{\sigma}{2g}}\left(\tan_{bp}(\sqrt{2\sigma}\Lambda) \pm \sqrt{bp}\sec_{bp}(\sqrt{2\sigma}\Lambda)\right),\\
H_{13}^{\pm}(\Lambda) &= \sqrt{\frac{\sigma}{2g}}\left(\cot_{bp}(\sqrt{2\sigma}\Lambda) \pm \sqrt{bp}\csc_{bp}(\sqrt{2\sigma}\Lambda)\right),\\
H_{14}^{\pm}(\Lambda) &= \sqrt{\frac{\sigma}{8g}}\left(\tan_{bp}(\sqrt{\frac{\sigma}{8}}\Lambda) + \cot_{bp}(\sqrt{\frac{\sigma}{8}}\Lambda)\right).
\end{aligned}
$$

$\mathrm{sech}_{bp}(\Lambda)$, $\tanh_{bp}(\Lambda)$, $\tan_{bp}(\Lambda)$, $\cot_{bp}(\Lambda)$, etc, are hyperbolic and generalized trigonometric functions with parameters b and p. When $b = p = 1$, they are recognized as hyperbolic and trigonometric functions.

Third step: The homogeneous balancing approach determines N.

Fourth step: Inserting Eqs (4.4) and (4.5) into Eq (4.3) yields a polynomial in H^i. Algebraic equations are generated by connecting all terms of similar power to zero. By solving the obtained system, we may determine the values of the unknowns.

5. Using the semi inverse variational method

This section's objective is to extract the Hamiltonian system and construct the variational principle using He's semi-inverse technique. For this, we introduce the transformation as:

$$u(x,t) = U(\Lambda)e^{\iota\eta(x,t)},\ v(x,t) = V(\Lambda),\ w(x,t) = W(\Lambda). \tag{5.1}$$

In this context, the wave variable Λ and phase component η are defined as follows:

$$
\begin{cases}
\Lambda = \dfrac{k_1 x^{\beta}}{\Gamma(1+\beta)} + \dfrac{k_2 t^{\alpha}}{\Gamma(1+\alpha)},\\
\eta = \dfrac{a_1 x^{\beta}}{\Gamma(1+\beta)} + \dfrac{a_2 t^{\alpha}}{\Gamma(1+\alpha)}.
\end{cases} \tag{5.2}
$$

Equation (1.1) is transformed into the following NODEs, by applying this transformation:

$$
\begin{cases}
(k_1k_2 - (k_1)^2)U'' + (a_1^2 - a_1a_2)U - \dfrac{2U^3}{1-h^2} - (V-W)U = 0,\\
V = \dfrac{-k_2U^2}{\Phi}, W = \dfrac{k_2U^2}{\chi},
\end{cases} \tag{5.3}
$$

where

$$
\begin{cases}
\Phi = (1+h)(k_2 - (1+h)k_1),\\
\chi = (1-h)(k_2 - (1-h)k_1).
\end{cases}
$$

The second part of Eq (5.3) is combined with the first component to create a single NODE for the system.

$$U'' + \frac{a_1(a_1 - a_2)U}{k_1(k_2 - k_1)} + \frac{2U^3}{(k_2 - k_1)^2 - k_1^2 h^2} = 0 \tag{5.4}$$

with the constraint from the imaginary part:

$$k_2 = \frac{k_2 a_1}{2a_1 - a_2}. \tag{5.5}$$

Its variational principle (VP) can be established by employing the semi inverse method as

$$J = \int_0^\infty \left[\frac{-1}{2} \left(\frac{dU}{d\Lambda} \right)^2 - \frac{(2a_1 - a_2)^2}{2k_2} U^2 - \frac{(2a_1 - a_2)^2}{2k_2^2 h^2 a_2^2} U^4 \right] d\Lambda = \int_0^\infty [v - p]\, d\Lambda. \tag{5.6}$$

The variational approach employed to construct solitary wave solutions is theoretically based on the obtained VP in Eq (5.6). Moreover, this approach can also be applied to derive the Hamiltonian:

$$L = v + p = \frac{-1}{2} \left(\frac{dU}{d\Lambda} \right)^2 + \frac{(2a_1 - a_2)^2}{2k_2} U^2 + \frac{(2a_1 - a_2)^2}{2k_2^2 h^2 a_2^2} U^4.$$

When v and p represent the system's kinetic and potential energies, respectively:

$$v = \frac{-1}{2} \left(\frac{dU}{d\Lambda} \right)^2, \tag{5.7}$$

$$p = \frac{(2a_1 - a_2)^2}{2k_2} U^2 + \frac{(2a_1 - a_2)^2}{2k_2^2 h^2 a_2^2} U^4. \tag{5.8}$$

The system's energy conservation is demonstrated through then shown via the Hamiltonian. Building on this foundation, we will extract the periodic wave solutions will be extracted in the subsequent analysis using the Hamiltonian-based approach.

5.1. The variational method

Family one:

$$U = A\ \mathrm{sech}(\Lambda). \tag{5.9}$$

Putting it into Eq (5.6) yields

$$\begin{aligned} J(A) &= \int_0^\infty \left[\frac{-1}{2} \left(\frac{dU}{d\Lambda} \right)^2 - \frac{(2a_1 - a_2)^2}{2k_2} U^2 - \frac{(2a_1 - a_2)^2}{2k_2^2 h^2 a_2^2} U^4 \right] d\Lambda \\ &= \int_0^\infty \left[\frac{-1}{2} (-A\ \mathrm{sech}(\Lambda) \tanh(\Lambda))^2 - \frac{(2a_1 - a_2)^2}{2k_2} [A\ \mathrm{sech}(\Lambda)]^2 - \frac{(2a_1 - a_2)^2}{2k_2^2 h^2 a_2^2} [A\ \mathrm{sech}(\Lambda)]^4 \right] d\Lambda \\ &= \frac{1}{6} \frac{A^2 (12h^2 a_1^2 a_2^2 k_2 - 12h^2 a_1 a_2^3 k_2 + 3h^2 a_2^4 k_2 - h^2 a_2^2 k_2^2 + 8A^2 a_1^2 - 8A^2 a_1 a_2 + 2A^2 a_2^2)}{(h^2 a_2^2 k_2^2)}. \end{aligned} \tag{5.10}$$

We use the Ritz method to determine its stationary condition, which is

$$\frac{dJ(A)}{dA} = 0. \tag{5.11}$$

Resolving it results in

$$A = \frac{1}{2}\frac{\sqrt{-12a_1^2k_2 + 12a_1a_2k_2 - 3a_2^2k_2 + k_2^2}\, a_2 h}{2a_1 - a_2}. \tag{5.12}$$

As a result, the solitary wave solution is obtained as

$$\begin{cases} u_1(x,t) = \dfrac{1}{2}\dfrac{\sqrt{-12a_1^2k_2 + 12a_1a_2k_2 - 3a_2^2k_2 + k_2^2}\, a_2 h}{2a_1 - a_2}\ \operatorname{sech}(\Lambda)e^{i\eta}, \\ v_1(x,t) = \dfrac{-k_2}{\Phi}\left(\dfrac{1}{2}\dfrac{\sqrt{-12a_1^2k_2 + 12a_1a_2k_2 - 3a_2^2k_2 + k_2^2}\, a_2 h}{2a_1 - a_2}\ \operatorname{sech}(\Lambda)\right)^2, \\ w_1(x,t) = \dfrac{k_2}{\chi}\left(\dfrac{1}{2}\dfrac{\sqrt{-12a_1^2k_2 + 12a_1a_2k_2 - 3a_2^2k_2 + k_2^2}\, a_2 h}{2a_1 - a_2}\ \operatorname{sech}(\Lambda)\right)^2. \end{cases} \tag{5.13}$$

Family two: Here we can set

$$U = \frac{A}{1 + \cosh(\Lambda)}. \tag{5.14}$$

When it is inserted into Eq (5.6), the result is

$$\begin{aligned} J(A) &= \int_0^\infty \left[\frac{-1}{2}\left(\frac{dU}{d\Lambda}\right)^2 - \frac{(2a_1 - a_2)^2}{2k_2}U^2 - \frac{(2a_1 - a_2)^2}{2k_2^2h^2a_2^2}U^4\right] d\Lambda \\ &= \int_0^\infty \left[\frac{-1}{2}\left(\frac{-A\sinh(\Lambda)}{[1+\cosh(\Lambda)]^2}\right)^2 - \frac{(2a_1-a_2)^2}{2k_2}\left[\frac{A}{1+\cosh(\Lambda)}\right]^2 - \frac{(2a_1-a_2)^2}{2k_2^2h^2a_2^2}\left[\frac{A}{1+\cosh(\Lambda)}\right]^4\right] d\Lambda \\ &= \frac{1}{20}\frac{A^2(140h^2a_1^2a_2^2k_2 - 140h^2a_1a_2^3k_2 + 35h^2a_2^4k_2 - 7h^2a_2^2k_2^2 + 24A^2a_1^2 - 24A^2a_1a_2 + 6A^2a_2^2)}{(h^2a_2^2k_2^2)}. \end{aligned} \tag{5.15}$$

We use the Ritz method to determine its stationary condition, which is

$$\frac{dJ(A)}{dA} = 0. \tag{5.16}$$

The solution leads to

$$A = \frac{1}{2}\frac{\sqrt{-\frac{140}{3}a_1^2k_2 + \frac{140}{3}a_1k_2a_2 - \frac{35}{3}a_2^2k_2 + \frac{7}{3}k_2^2}\, a_2 h}{2a_1 - a_2}. \tag{5.17}$$

As a result, the solitary wave solution is obtained as

$$\begin{cases} u_2(x,t) = \dfrac{\left(\dfrac{1}{2}\dfrac{\sqrt{-\frac{140}{3}a_1^2k_2+\frac{140}{3}a_1k_2a_2-\frac{35}{3}a_2^2k_2+\frac{7}{3}k_2^2}\,a_2h}{2a_1-a_2}\right)}{1+\cosh(\Lambda)}e^{i\eta}, \\ v_2(x,t) = \dfrac{-k_2}{\Phi}\left(\dfrac{\frac{1}{2}\dfrac{\sqrt{-\frac{140}{3}a_1^2k_2+\frac{140}{3}a_1k_2a_2-\frac{35}{3}a_2^2k_2+\frac{7}{3}k_2^2}\,a_2h}{2a_1-a_2}}{1+\cosh(\Lambda)}\right)^2, \\ w_2(x,t) = \dfrac{k_2}{\chi}\left(\dfrac{\frac{1}{2}\dfrac{\sqrt{-\frac{140}{3}a_1^2k_2+\frac{140}{3}a_1k_2a_2-\frac{35}{3}a_2^2k_2+\frac{7}{3}k_2^2}\,a_2h}{2a_1-a_2}}{1+\cosh(\Lambda)}\right)^2. \end{cases} \tag{5.18}$$

Family three:

$$U = A\ \operatorname{sech}^2(\Lambda). \tag{5.19}$$

Inserting it into Eq (5.6) yields:

$$\begin{aligned} J(A) &= \int_0^\infty \left[\frac{-1}{2}\left(\frac{dU}{d\Lambda}\right)^2 - \frac{(2a_1-a_2)^2}{2k_2}U^2 - \frac{(2a_1-a_2)^2}{2k_2^2h^2a_2^2}U^4\right]d\Lambda \\ &= \int_0^\infty \left[\frac{-1}{2}\left(-2A\operatorname{sech}^2(\Lambda)\tanh(\Lambda)\right)^2 - \frac{(2a_1-a_2)^2}{2k_2}[A\operatorname{sech}^2(\Lambda)]^2 - \frac{(2a_1-a_2)^2}{2k_2^2h^2a_2^2}[A\operatorname{sech}^2(\Lambda)]^4\right]d\Lambda \\ &= \frac{1}{105}\frac{A^2(140h^2a_1^2a_2^2k_2-140h^2a_1a_2^3k_2+35h^2a_2^4k_2-28h^2a_2^2k_2^2+96A^2a_1^2-96A^2a_1a_2+24A^2a_2^2)}{(h^2a_2^2k_2^2)}. \end{aligned} \tag{5.20}$$

We determine its stationary condition using the Ritz approach as follows:

$$\frac{dJ(A)}{dA} = 0. \tag{5.21}$$

Solving it leads

$$A = \frac{1}{4}\frac{\sqrt{\frac{-140}{3}a_1^2k_2+\frac{140}{3}a_1a_2k_2-\frac{35}{3}a_2^2k_2+\frac{28}{3}k_2^2}\,a_2h}{2a_1-a_2}. \tag{5.22}$$

Thus, the solution for a solitary wave is obtained as

$$\begin{cases} u_3(x,t) = \dfrac{1}{4}\dfrac{\sqrt{\frac{-140}{3}a_1^2k_2 + \frac{140}{3}a_1a_2k_2 - \frac{35}{3}a_2^2k_2 + \frac{28}{3}k_2^2}\, a_2h}{2a_1 - a_2}\ \operatorname{sech}(\Lambda)^2 e^{i\eta}, \\ v_3(x,t) = \dfrac{-k_2}{\Phi}\left(\dfrac{1}{4}\dfrac{\sqrt{\frac{-140}{3}a_1^2k_2 + \frac{140}{3}a_1a_2k_2 - \frac{35}{3}a_2^2k_2 + \frac{28}{3}k_2^2}\, a_2h}{2a_1 - a_2}\ \operatorname{sech}(\Lambda)^2\right)^2, \\ w_3(x,t) = \dfrac{k_2}{\chi}\left(\dfrac{1}{4}\dfrac{\sqrt{\frac{-140}{3}a_1^2k_2 + \frac{140}{3}a_1a_2k_2 - \frac{35}{3}a_2^2k_2 + \frac{28}{3}k_2^2}\, a_2h}{2a_1 - a_2}\ \operatorname{sech}(\Lambda)^2\right)^2, \end{cases} \tag{5.23}$$

where Λ and η are defined in Eq (5.2).

5.2. The Hamiltonian-based method

$$U = A\ \cos(B\Lambda),\ B > 0, \tag{5.24}$$

where A and B are the frequency and amplitude, respectively. Taking into account the system's Hamiltonian Eq (5.4):

$$L = v + p = \frac{-1}{2}\left(\frac{dU}{d\Lambda}\right)^2 + \frac{(2a_1 - a_2)^2}{2k_2}U^2 + \frac{(2a_1 - a_2)^2}{2k_2^2h^2a_2^2}U^4. \tag{5.25}$$

Energy conservation theory tells us that the system's total energy stays constant as

$$L = v + p = \frac{-1}{2}\left(\frac{dU}{d\Lambda}\right)^2 + \frac{(2a_1 - a_2)^2}{2k_2}U^2 + \frac{(2a_1 - a_2)^2}{2k_2^2h^2a_2^2}U^4 = L_0, \tag{5.26}$$

where the Hamiltonian constant is denoted by L_0.

By establishing

$$\Lambda = 0, \tag{5.27}$$

for Eq (5.24), then inserting the findings into Eq (5.26) produces

$$L_0 = \frac{(2a_1 - a_2)^2}{2k_2}A^2 + \frac{(2a_1 - a_2)^2}{2k_2^2h^2a_2^2}A^4. \tag{5.28}$$

When Eq (5.24) is inserted into Eq (5.26), the result is

$$\begin{aligned} L =& \frac{-1}{2}[-AB\ \sin(B\Lambda)]^2 + \frac{(2a_1 - a_2)^2}{2k_2}[A\ \cos(B\Lambda)]^2 + \frac{(2a_1 - a_2)^2}{2k_2^2h^2a_2^2}[A\ \cos(B\Lambda)]^4 \\ =& L_0 = \frac{(2a_1 - a_2)^2}{2k_2}A^2 + \frac{(2a_1 - a_2)^2}{2k_2^2h^2a_2^2}A^4. \end{aligned} \tag{5.29}$$

Now we can set

$$B\Lambda = \frac{\pi}{4}. \tag{5.30}$$

Then, there is

$$\frac{-1}{4}A^2B^2 + \frac{(2a_1 - a_2)^2}{4k_2}A^2 + \frac{(2a_1 - a_2)^2}{32k_2^2h^2a_2^2} = \frac{(2a_1 - a_2)^2}{2k_2}A^2 + \frac{(2a_1 - a_2)^2}{2k_2^2h^2a_2^2}A^4. \tag{5.31}$$

Solving it, we have

$$B = \frac{1}{2}\frac{\sqrt{-4h^2a_2^2k_2 - 6A^2}(2a_1 - a_2)}{(k_2a_2h)}, \tag{5.32}$$

$$\begin{cases} u_4(x,t) = A\ \cos\left(\frac{1}{2}\frac{\sqrt{-4h^2a_2^2k_2 - 6A^2}(2a_1 - a_2)}{(k_2a_2h)}\Lambda\right)e^{i\eta}, \\ v_4(x,t) = \frac{-k_2}{\Phi}\left(A\ \cos\left(\frac{1}{2}\frac{\sqrt{-4h^2a_2^2k_2 - 6A^2}(2a_1 - a_2)}{(k_2a_2h)}\Lambda\right)\right)^2, \\ w_4(x,t) = \frac{k_2}{\chi}\left(A\ \cos\left(\frac{1}{2}\frac{\sqrt{-4h^2a_2^2k_2 - 6A^2}(2a_1 - a_2)}{(k_2a_2h)}\Lambda\right)\right)^2, \end{cases} \tag{5.33}$$

where Λ and η are defined in Eq (5.2).

6. Utilization of Sardar sub-equation method

In Eq (5.4), balancing U'' with U^3 yields $R = 1$. The solution of Eq (5.4) can be written as

$$U(\Lambda) = q_0 + q_1H(\Lambda). \tag{6.1}$$

Applying the proposed technique, following set of solutions has been obtained:

$$q_0 = 0,\ q_1 = \frac{\sqrt{-a_1^2g(a_1 - a_2)^2 + g\sigma^2h^2k_1^4}}{ok_1},\ k_1 = \frac{a_1(a_2 - a_1)}{\sigma k_1} + k_2. \tag{6.2}$$

Case 1: When $\sigma > 0$ and $c = 0$, then

$$\begin{cases} u_1^{\pm}(x,t) = \sqrt{-\frac{bp\sigma}{g}}\ \frac{\sqrt{-a_1^2g(a_1 - a_2)^2 + g\sigma^2h^2k_1^4}}{\sigma k_1}\ \mathrm{sech}\left(\sqrt{\sigma}\Lambda\right)e^{\iota\eta(x,t)}, \quad g < 0, \\ v_1^{\pm}(x,t) = \frac{-k_2}{\Phi}\left(\sqrt{-\frac{bp\sigma}{g}}\ \frac{\sqrt{-a_1^2g(a_1 - a_2)^2 + g\sigma^2h^2k_1^4}}{\sigma k_1}\ \mathrm{sech}\left(\sqrt{\sigma}\Lambda\right)\right)^2, \quad g < 0, \\ w_1^{\pm}(x,t) = \frac{k_2}{\chi}\left(\sqrt{-\frac{bp\sigma}{g}}\ \frac{\sqrt{-a_1^2g(a_1 - a_2)^2 + g\sigma^2h^2k_1^4}}{\sigma k_1}\ \mathrm{sech}\left(\sqrt{\sigma}\Lambda\right)\right)^2, \quad g < 0. \end{cases}$$

$$\begin{cases} u_2^{\pm}(x,t) = \sqrt{\dfrac{bp\sigma}{g}}\ \dfrac{\sqrt{-a_1^2 g(a_1-a_2)^2 + g\sigma^2 h^2 k_1^4}}{\sigma k_1}\ \operatorname{csch}\left(\sqrt{\sigma}\Lambda\right) e^{\iota\eta(x,t)}, \quad g>0, \\ v_2^{\pm}(x,t) = \dfrac{-k_2}{\Phi}\left(\sqrt{\dfrac{bp\sigma}{g}}\ \dfrac{\sqrt{-a_1^2 g(a_1-a_2)^2 + g\sigma^2 h^2 k_1^4}}{\sigma k_1}\ \operatorname{csch}\left(\sqrt{\sigma}\Lambda\right)\right)^2, \quad g>0, \\ w_2^{\pm}(x,t) = \dfrac{k_2}{\chi}\left(\sqrt{\dfrac{bp\sigma}{g}}\ \dfrac{\sqrt{-a_1^2 g(a_1-a_2)^2 + g\sigma^2 h^2 k_1^4}}{\sigma k_1}\ \operatorname{csch}\left(\sqrt{\sigma}\Lambda\right)\right)^2, \quad g>0. \end{cases}$$

Case 2: If $\sigma < 0$, $g > 0$, and $c = 0$, then

$$\begin{cases} u_3^{\pm}(x,t) = \sqrt{-\dfrac{bp\sigma}{g}}\ \dfrac{\sqrt{-a_1^2 g(a_1-a_2)^2 + g\sigma^2 h^2 k_1^4}}{\sigma k_1}\ \sec\left(\sqrt{-\sigma}\Lambda\right) e^{\iota\eta(x,t)}, \\ v_3^{\pm}(x,t) = \dfrac{-k_2}{\Phi}\left(\sqrt{-\dfrac{bp\sigma}{g}}\ \dfrac{\sqrt{-a_1^2 g(a_1-a_2)^2 + g\sigma^2 h^2 k_1^4}}{\sigma k_1}\ \sec\left(\sqrt{-\sigma}\Lambda\right)\right)^2, \\ w_3^{\pm}(x,t) = \dfrac{k_2}{\chi}\left(\sqrt{-\dfrac{bp\sigma}{g}}\ \dfrac{\sqrt{-a_1^2 g(a_1-a_2)^2 + g\sigma^2 h^2 k_1^4}}{\sigma k_1}\ \sec\left(\sqrt{-\sigma}\Lambda\right)\right)^2. \end{cases}$$

$$\begin{cases} u_4^{\pm}(x,t) = \sqrt{-\dfrac{bp\sigma}{g}}\ \dfrac{\sqrt{-a_1^2 g(a_1-a_2)^2 + g\sigma^2 h^2 k_1^4}}{\sigma k_1}\ \csc\left(\sqrt{-\sigma}\Lambda\right) e^{\iota\eta(x,t)}, \\ v_4^{\pm}(x,t) = \dfrac{-k_2}{\Phi}\left(\sqrt{-\dfrac{bp\sigma}{g}}\ \dfrac{\sqrt{-a_1^2 g(a_1-a_2)^2 + go^2 h^2 k_1^4}}{ok_1}\ \csc\left(\sqrt{-o}\Lambda\right)\right)^2, \\ w_4^{\pm}(x,t) = \dfrac{k_2}{\chi}\left(\sqrt{-\dfrac{bp\sigma}{g}}\ \dfrac{\sqrt{-a_1^2 g(a_1-a_2)^2 + g\sigma^2 h^2 k_1^4}}{\sigma k_1}\ \csc\left(\sqrt{-\sigma}\Lambda\right)\right)^2. \end{cases}$$

Case 3: If $\sigma < 0$, $g > 0$ and $c = \frac{\sigma^2}{4g}$, then

$$\begin{cases} u_5^{\pm}(x,t) = \sqrt{\dfrac{-\sigma}{2g}}\ \dfrac{\sqrt{-a_1^2 g(a_1-a_2)^2 + g\sigma^2 h^2 k_1^4}}{\sigma k_1}\ \tanh\left(\sqrt{\dfrac{-\sigma}{2}}\Lambda\right) e^{\iota\eta(x,t)}, \\ v_5^{\pm}(x,t) = \dfrac{-k_2}{\Phi}\left(\sqrt{\dfrac{-\sigma}{2g}}\ \dfrac{\sqrt{-a_1^2 g(a_1-a_2)^2 + g\sigma^2 h^2 k_1^4}}{\sigma k_1}\ \tanh\left(\sqrt{\dfrac{-\sigma}{2}}\Lambda\right)\right)^2, \\ w_5^{\pm}(x,t) = \dfrac{k_2}{\chi}\left(\sqrt{\dfrac{-\sigma}{2g}}\ \dfrac{\sqrt{-a_1^2 g(a_1-a_2)^2 + g\sigma^2 h^2 k_1^4}}{\sigma k_1}\ \tanh\left(\sqrt{\dfrac{-\sigma}{2}}\Lambda\right)\right)^2. \end{cases}$$

$$\begin{cases} u_6^{\pm}(x,t) = \sqrt{\dfrac{-\sigma}{2g}}\dfrac{\sqrt{-a_1^2g(a_1-a_2)^2+g\sigma^2h^2k_1^4}}{\sigma k_1}\coth(\sqrt{\dfrac{-\sigma}{2}}\Lambda)e^{\iota\eta(x,t)}, \\ v_6^{\pm}(x,t) = \dfrac{-k_2}{\Phi}\left(\sqrt{\dfrac{-\sigma}{2g}}\dfrac{\sqrt{-a_1^2g(a_1-a_2)^2+g\sigma^2h^2k_1^4}}{\sigma k_1}\coth(\sqrt{\dfrac{-\sigma}{2}}\Lambda)\right)^2, \\ w_6^{\pm}(x,t) = \dfrac{k_2}{\chi}\left(\sqrt{\dfrac{-\sigma}{2g}}\dfrac{\sqrt{-a_1^2g(a_1-a_2)^2+g\sigma^2h^2k_1^4}}{\sigma k_1}\coth(\sqrt{\dfrac{-\sigma}{2}}\Lambda)\right)^2. \end{cases}$$

$$\begin{cases} u_7^{\pm}(x,t) = \sqrt{\dfrac{-o}{2g}}\dfrac{\sqrt{-a_1^2g(a_1-a_2)^2+go^2h^2k_1^4}}{ok_1}\left(\tanh(\sqrt{-2o}\Lambda)\pm\iota\sqrt{bp}\,\mathrm{sech}(\sqrt{-2o}\Lambda)\right)e^{\iota\eta(x,t)}, \\ v_7^{\pm}(x,t) = \dfrac{-k_2}{\Phi}\left(\sqrt{\dfrac{-o}{2g}}\dfrac{\sqrt{-a_1^2g(a_1-a_2)^2+go^2h^2k_1^4}}{ok_1}\left(\tanh(\sqrt{-2o}\Lambda)\pm\iota\sqrt{bp}\,\mathrm{sech}(\sqrt{-2o}\Lambda)\right)\right)^2, \\ w_7^{\pm}(x,t) = \dfrac{k_2}{\chi}\left(\sqrt{\dfrac{-o}{2g}}\dfrac{\sqrt{-a_1^2g(a_1-a_2)^2+go^2h^2k_1^4}}{ok_1}\left(\tanh(\sqrt{-2o}\Lambda)\pm\iota\sqrt{bp}\,\mathrm{sech}(\sqrt{-2o}\Lambda)\right)\right)^2. \end{cases}$$

$$\begin{cases} u_8^{\pm}(x,t) = \sqrt{\dfrac{-o}{2g}}\dfrac{\sqrt{-a_1^2g(a_1-a_2)^2+go^2h^2k_1^4}}{ok_1}\sqrt{\dfrac{-o}{2g}}\left(\coth(\sqrt{-2o}\Lambda)\pm\sqrt{bp}\,\mathrm{csch}(\sqrt{-2o}\Lambda)\right)e^{\iota\eta(x,t)}, \\ v_8^{\pm}(x,t) = \dfrac{-k_2}{\Phi}\left(\sqrt{\dfrac{-o}{2g}}\dfrac{\sqrt{-a_1^2g(a_1-a_2)^2+go^2h^2k_1^4}}{ok_1}\left(\coth(\sqrt{-2o}\Lambda)\pm\sqrt{bp}\,\mathrm{csch}(\sqrt{-2o}\Lambda)\right)\right)^2, \\ w_8^{\pm}(x,t) = \dfrac{k_2}{\chi}\left(\sqrt{\dfrac{-o}{2g}}\dfrac{\sqrt{-a_1^2g(a_1-a_2)^2+go^2h^2k_1^4}}{ok_1}\left(\coth(\sqrt{-2o}\Lambda)\pm\sqrt{bp}\,\mathrm{csch}(\sqrt{-2o}\Lambda)\right)\right)^2. \end{cases}$$

$$\begin{cases} u_9^{\pm}(x,t) = \pm\sqrt{\dfrac{-o}{8g}}\dfrac{\sqrt{-a_1^2g(a_1-a_2)^2+go^2h^2k_1^4}}{ok_1}\left(\tanh(\sqrt{\dfrac{-o}{8}}\Lambda)+\coth(\sqrt{\dfrac{-o}{8}}\Lambda)\right)e^{\iota\eta(x,t)}, \\ v_9^{\pm}(x,t) = \dfrac{-k_2}{\Phi}\pm\sqrt{\dfrac{-o}{8g}}\left(\dfrac{\sqrt{-a_1^2g(a_1-a_2)^2+go^2h^2k_1^4}}{ok_1}\left(\tanh(\sqrt{\dfrac{-o}{8}}\Lambda)+\coth(\sqrt{\dfrac{-o}{8}}\Lambda)\right)\right)^2, \\ w_9^{\pm}(x,t) = \dfrac{k_2}{\chi}\pm\sqrt{\dfrac{-o}{8g}}\left(\dfrac{\sqrt{-a_1^2g(a_1-a_2)^2+go^2h^2k_1^4}}{ok_1}\left(\tanh(\sqrt{\dfrac{-o}{8}}\Lambda)+\coth(\sqrt{\dfrac{-o}{8}}\Lambda)\right)\right)^2. \end{cases}$$

Case 4: If $\sigma > 0$, $g > 0$ and $c = \frac{\sigma^2}{4g}$, then

$$\begin{cases} u_{10}^{\pm}(x,t) = \sqrt{\dfrac{\sigma}{2g}}\dfrac{\sqrt{-a_1^2g(a_1-a_2)^2+g\sigma^2h^2k_1^4}}{\sigma k_1}\tan(\sqrt{\dfrac{\sigma}{2}}\Lambda)e^{\iota\eta(x,t)}, \\ v_{10}^{\pm}(x,t) = \dfrac{-k_2}{\Phi}\left(\sqrt{\dfrac{\sigma}{2g}}\dfrac{\sqrt{-a_1^2g(a_1-a_2)^2+g\sigma^2h^2k_1^4}}{\sigma k_1}\tan(\sqrt{\dfrac{\sigma}{2}}\Lambda)\right)^2, \\ w_{10}^{\pm}(x,t) = \dfrac{k_2}{\chi}\left(\sqrt{\dfrac{\sigma}{2g}}\dfrac{\sqrt{-a_1^2g(a_1-a_2)^2+g\sigma^2h^2k_1^4}}{\sigma k_1}\tan(\sqrt{\dfrac{\sigma}{2}}\Lambda)\right)^2. \end{cases}$$

$$\begin{cases} u_{11}^{\pm}(x,t) = \sqrt{\dfrac{\sigma}{2g}}\dfrac{\sqrt{-a_1^2g(a_1-a_2)^2+g\sigma^2h^2k_1^4}}{\sigma k_1}\cot(\sqrt{\dfrac{\sigma}{2}}\Lambda)e^{\iota\eta(x,t)}, \\ v_{11}^{\pm}(x,t) = \dfrac{-k_2}{\Phi}\left(\sqrt{\dfrac{\sigma}{2g}}\dfrac{\sqrt{-a_1^2g(a_1-a_2)^2+g\sigma^2h^2k_1^4}}{\sigma k_1}\cot(\sqrt{\dfrac{\sigma}{2}}\Lambda)\right)^2, \\ w_{11}^{\pm}(x,t) = \dfrac{k_2}{\chi}\left(\sqrt{\dfrac{\sigma}{2g}}\dfrac{\sqrt{-a_1^2g(a_1-a_2)^2+g\sigma^2h^2k_1^4}}{\sigma k_1}\cot(\sqrt{\dfrac{\sigma}{2}}\Lambda)\right)^2. \end{cases}$$

$$\begin{cases} u_{12}^{\pm}(x,t) = \sqrt{\dfrac{\sigma}{2g}}\dfrac{\sqrt{-a_1^2g(a_1-a_2)^2+g\sigma^2h^2k_1^4}}{\sigma k_1}\left(\tan(\sqrt{2o}\Lambda)\pm\sqrt{bp}\sec(\sqrt{2\sigma}\Lambda)\right)e^{\iota\eta(x,t)}, \\ v_{12}^{\pm}(x,t) = \dfrac{-k_2}{\Phi}\left(\sqrt{\dfrac{\sigma}{2g}}\dfrac{\sqrt{-a_1^2g(a_1-a_2)^2+g\sigma^2h^2k_1^4}}{\sigma k_1}\left(\tan(\sqrt{2\sigma}\Lambda)\pm\sqrt{bp}\sec(\sqrt{2o}\Lambda)\right)\right)^2, \\ w_{12}^{\pm}(x,t) = \dfrac{k_2}{\chi}\left(\sqrt{\dfrac{\sigma}{2g}}\dfrac{\sqrt{-a_1^2g(a_1-a_2)^2+g\sigma^2h^2k_1^4}}{\sigma k_1}\left(\tan(\sqrt{2\sigma}\Lambda)\pm\sqrt{bp}\sec(\sqrt{2\sigma}\Lambda)\right)\right)^2. \end{cases}$$

$$\begin{cases} u_{13}^{\pm}(x,t) = \sqrt{\dfrac{\sigma}{2g}}\dfrac{\sqrt{-a_1^2g(a_1-a_2)^2+g\sigma^2h^2k_1^4}}{ak_1}\left(\cot_(\sqrt{2\sigma}\Lambda)\pm\sqrt{bp}\csc(\sqrt{2\sigma}\Lambda)\right)e^{\iota\eta(x,t)}, \\ v_{13}^{\pm}(x,t) = \dfrac{-k_2}{\Phi}\left(\sqrt{\dfrac{\sigma}{2g}}\dfrac{\sqrt{-a_1^2g(a_1-a_2)^2+g\sigma^2h^2k_1^4}}{ak_1}\left(\cot_(\sqrt{2\sigma}\Lambda)\pm\sqrt{bp}\csc(\sqrt{2\sigma}\Lambda)\right)\right)^2, \\ w_{13}^{\pm}(x,t) = \dfrac{k_2}{\chi}\left(\sqrt{\dfrac{\sigma}{2g}}\dfrac{\sqrt{-a_1^2g(a_1-a_2)^2+g\sigma^2h^2k_1^4}}{ak_1}\left(\cot_(\sqrt{2\sigma}\Lambda)\pm\sqrt{bp}\csc(\sqrt{2\sigma}\Lambda)\right)\right)^2. \end{cases}$$

$$\begin{cases} u_{14}^{\pm}(x,t) = \sqrt{\dfrac{\sigma}{8g}}\dfrac{\sqrt{-a_1^2 g(a_1-a_2)^2 + g\sigma^2 h^2 k_1^4}}{\sigma k_1}\left(\tan(\sqrt{\dfrac{\sigma}{8}}\Lambda) + \cot(\sqrt{\dfrac{\sigma}{8}}\Lambda)\right)e^{\iota\eta(x,t)}, \\ v_{14}^{\pm}(x,t) = \dfrac{-k_2}{\Phi}\left(\sqrt{\dfrac{\sigma}{8g}}\dfrac{\sqrt{-a_1^2 g(a_1-a_2)^2 + go^2 h^2 k_1^4}}{\sigma k_1}\left(\tan(\sqrt{\dfrac{o}{8}}\Lambda) + \cot(\sqrt{\dfrac{\sigma}{8}}\Lambda)\right)\right)^2, \\ w_{14}^{\pm}(x,t) = \dfrac{k_2}{\chi}\left(\sqrt{\dfrac{\sigma}{8g}}\dfrac{\sqrt{-a_1^2 g(a_1-a_2)^2 + g\sigma^2 h^2 k_1^4}}{\sigma k_1}\left(\tan(\sqrt{\dfrac{\sigma}{8}}\Lambda) + \cot(\sqrt{\dfrac{\sigma}{8}}\Lambda)\right)\right)^2, \end{cases}$$

where Λ and η are taken from Eq (5.2).

7. Graphical representations

This section elaborates on the physical characteristics and presents visual representations of the triple nonlinear fractional Schrödinger equation. The equation is examined under spatio-temporal effects. The discussion focuses on two highly effective methods: the Sardar subequation method and the semi-inverse variational method. These methods advances in obtaining soliton solutions and not previously been applied to this model before. To assess the fractional impact on the specific solutions of $u_1(x,t)$, $u_2(x,t)$, $u_4(x,t)$, $u_1^{\pm}(x,t)$, and $u_5^{\pm}(x,t)$, it involves $3D$ and $2D$ graphical representations, revealing behavior with specific parameter values for real components. The parameters α, β introduce adjustable dispersion and nonlinearity effects, where larger α slows energy dispersion, broadening solitons, while variations in β influence nonlinear interactions, altering soliton stability and dynamics. This approach effectively models fractional soliton behaviors. The $3D$ plots usually spatiotemporal evolution of the wave profile, demonstrating how the solution changes concurrently with space x and time t. $2D$ plots of solutions $u_1(x,t)$, $u_2(x,t)$, $u_4(x,t)$, $u_1^{\pm}(x,t)$, and $u_5^{\pm}(x,t)$ are displayed $t = 1$, $t = 2$ and $t = 3$ to illustrate wave propagation with fractional orders α and β fixed.

For $\alpha = 0.75$, $\beta = 0.75$, $\alpha = 0.95$, $\beta = 0.95$, and $\alpha = 1$, $\beta = 1$, the physical behaviors of real parts of U_1 are plotted in Figure 1 for $\alpha = 0.75$, $\beta = 0.75$, $\alpha = 0.95$, $\beta = 0.95$ and $\alpha = 1$, $\beta = 1$, allowing us to generate the bright-solitary wave. To illustrate wave propagation with fractional orders α and β fixed, line plots of solutions $u_1(x,t)$are presented as $t = 1$, $t = 2$, and $t = 3$, as indicated in legend of Figure 1.

For the parameters as $h = 1$, $a_1 = 1$, $a_2 = 1$, $k_1 = 2$, $k_2 = 2$, the behaviors of $Re[U_2]$ is plotted in Figure 2, which depicts bright solitons. To illustrate the wave propagation with fractional orders α and β fixed, line plots of solutions $Re[u_2(x,t)]$ are presented at $t = 1$, $t = 2$, and $t = 3$,as indicated in the legend of Figure 2.

If we use $A = \frac{1}{2}$, $h = 1$, $a_1 = 1$, $a_2 = 1, k_1 = 2$, $k_2 = 2$ for different fractional values at $\alpha = 0.75$, $\beta = 0.75$, $\alpha = 0.95$, $\beta = 0.95$, and $\alpha = 1$, $\beta = 1$. Figure 3 plots the performances of $Re[u_4(x,t)]$. The resulting waveform exhibits a perfectly periodic structure. Line graphs of $Re[u_4(x,t)]$ plotted at $t = 1$, $t = 2$, and $t = 3$, as indicated in the legend of Figure 3.

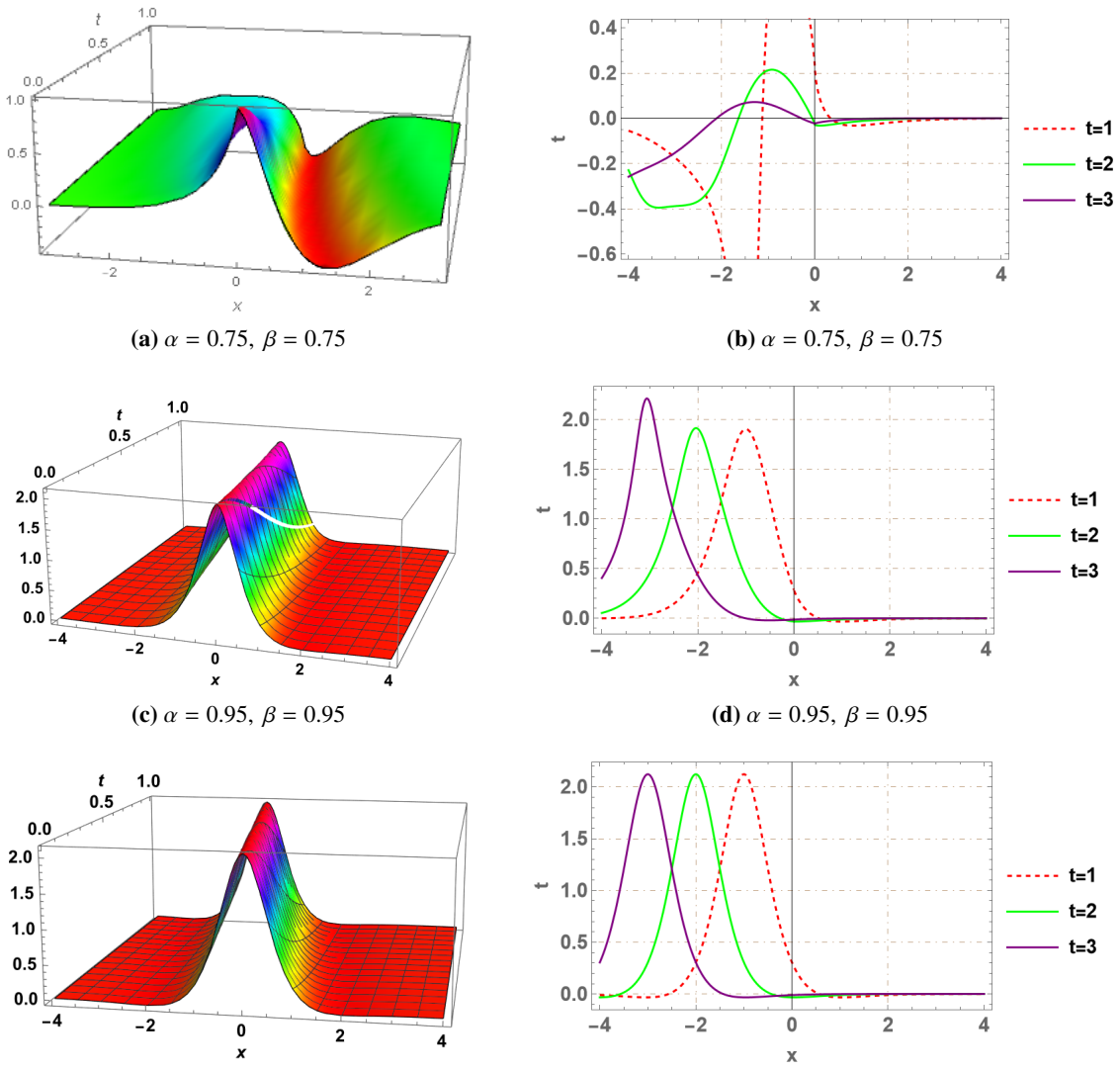

(a) $\alpha = 0.75,\ \beta = 0.75$ **(b)** $\alpha = 0.75,\ \beta = 0.75$

(c) $\alpha = 0.95,\ \beta = 0.95$ **(d)** $\alpha = 0.95,\ \beta = 0.95$

(e) $\alpha = 1,\ \beta = 1$ **(f)** $\alpha = 1,\ \beta = 1$

Figure 1. Physical presentation of $Re[u_1(x,t)]$.

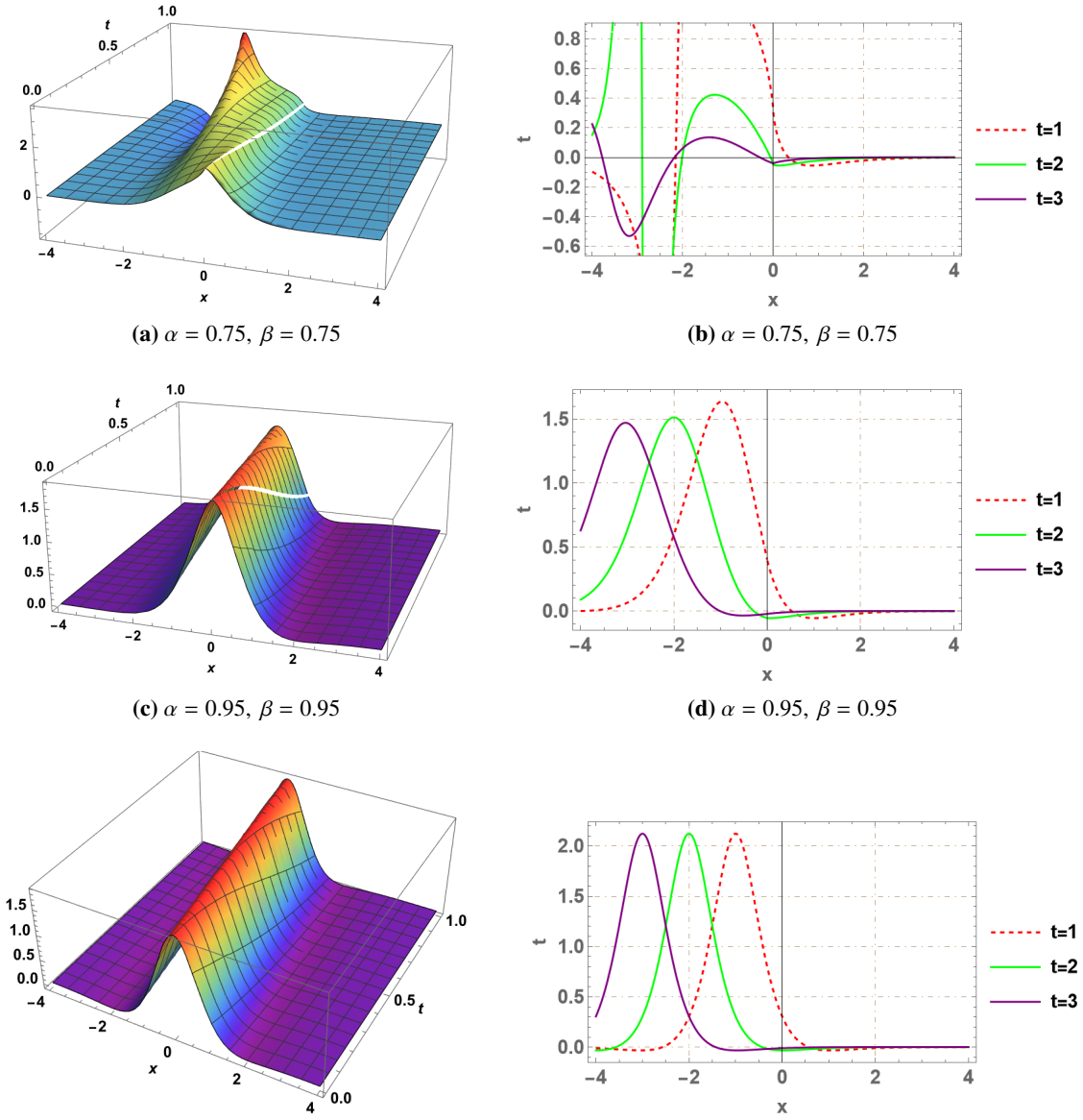

(a) $\alpha = 0.75,\ \beta = 0.75$ **(b)** $\alpha = 0.75,\ \beta = 0.75$

(c) $\alpha = 0.95,\ \beta = 0.95$ **(d)** $\alpha = 0.95,\ \beta = 0.95$

(e) $\alpha = 1,\ \beta = 1$ **(f)** $\alpha = 1,\ \beta = 1$

Figure 2. Graphical representation of $Re[u_2(x,t)]$.

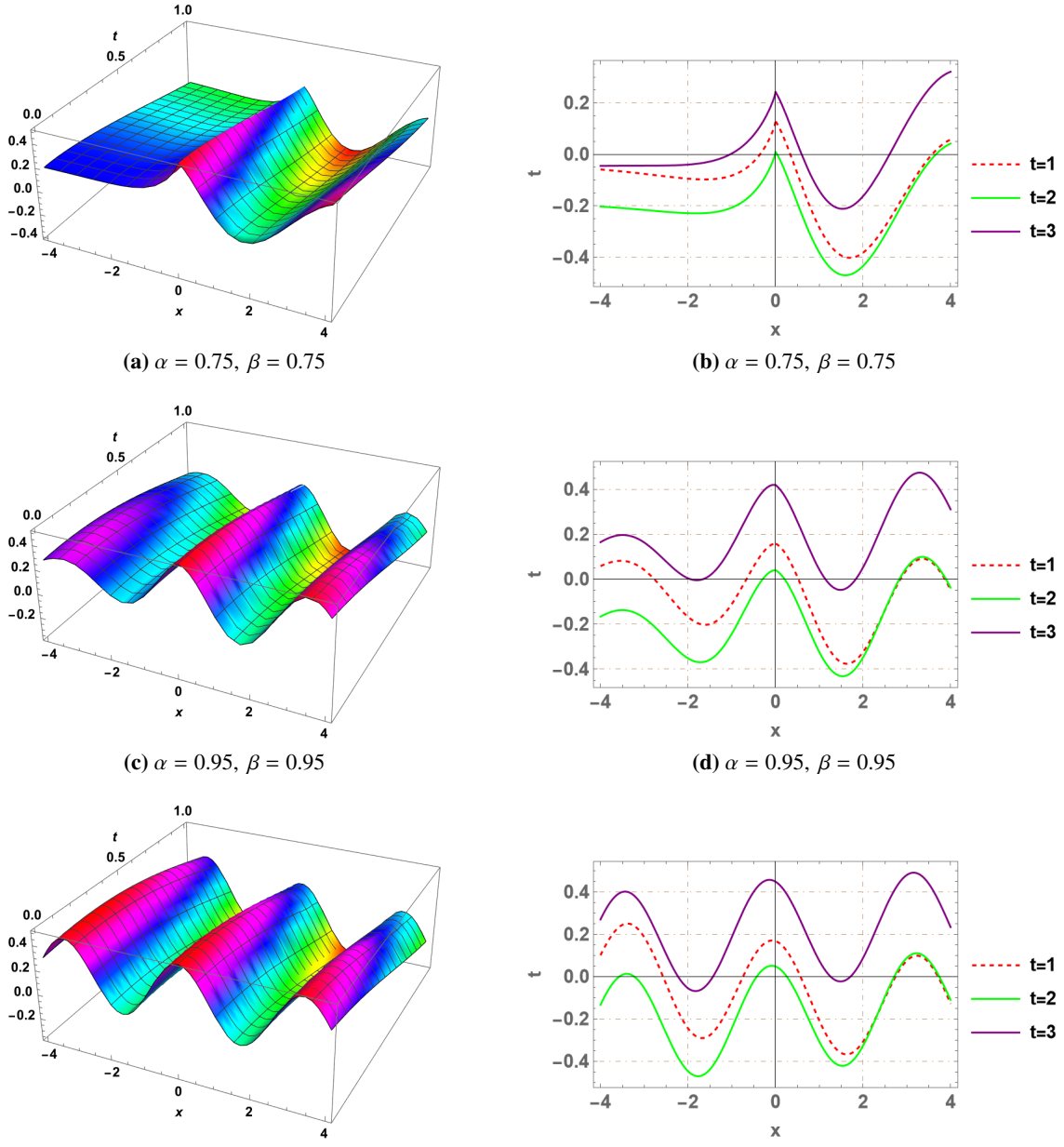

(a) $\alpha = 0.75,\ \beta = 0.75$ **(b)** $\alpha = 0.75,\ \beta = 0.75$

(c) $\alpha = 0.95,\ \beta = 0.95$ **(d)** $\alpha = 0.95,\ \beta = 0.95$

(e) $\alpha = 1,\ \beta = 1$ **(f)** $\alpha = 1,\ \beta = 1$

Figure 3. Graphical representation of $Re[u_4(x,t)]$.

The $3D$ and $2D$ graphs of the real parts of the solutions $u_1^{\pm}(x,t)$ by assigning different parameter values, such as $b = 1$, $p = 1$, $v = 2$, $k_2 = 1$, $o = 1$, $h = 0.1$, $k_1 = 3$, $a_1 = 5$, $a_2 = 2$, $g = -1$ are presented in Figure 4. Line graphs of $u_1^{\pm}(x,t)$ has been plotted for $t = 1$, $t = 2$, and $t = 3$, as indicated by the legend in Figure 4.

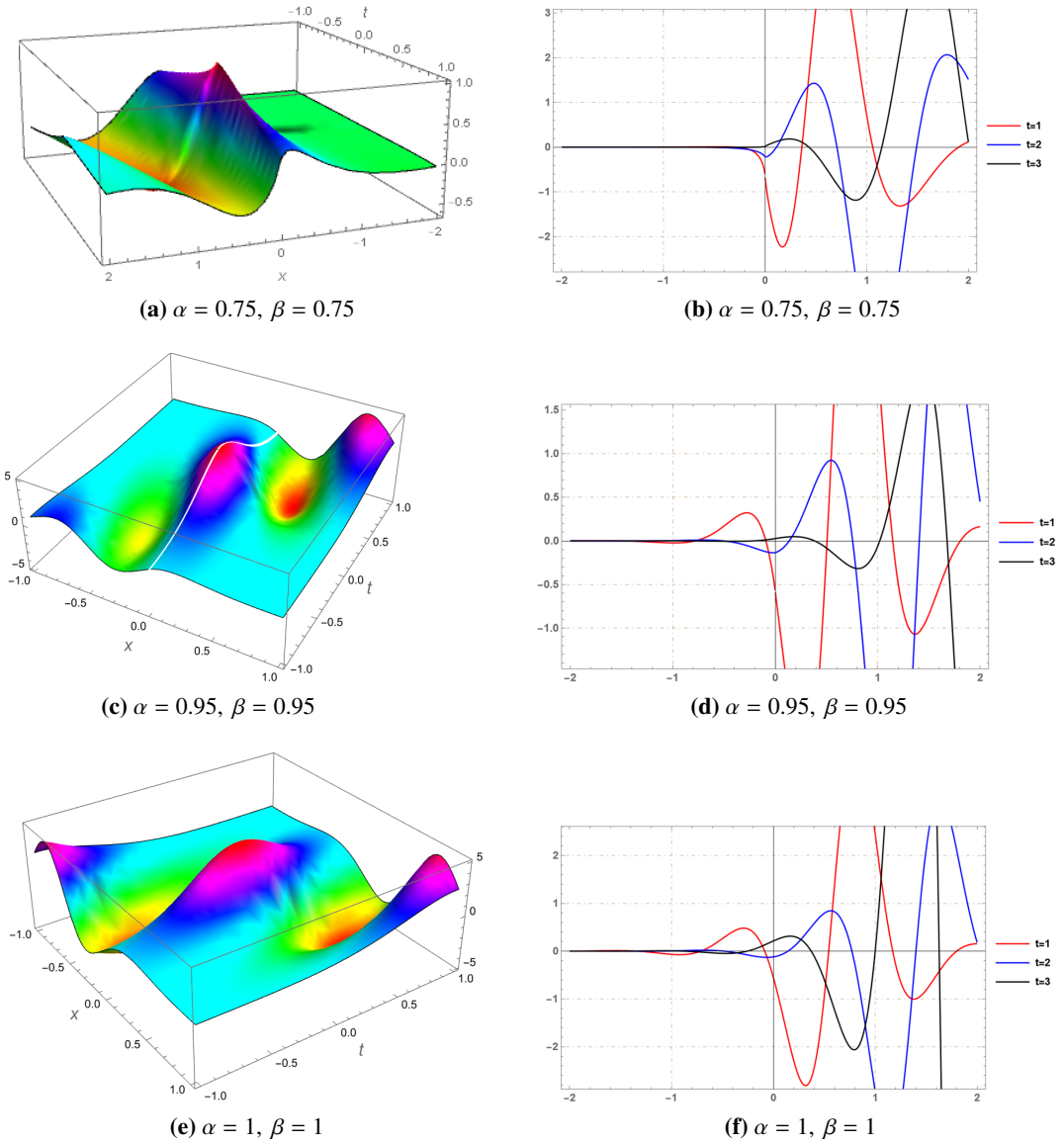

(a) $\alpha = 0.75$, $\beta = 0.75$ **(b)** $\alpha = 0.75$, $\beta = 0.75$

(c) $\alpha = 0.95$, $\beta = 0.95$ **(d)** $\alpha = 0.95$, $\beta = 0.95$

(e) $\alpha = 1$, $\beta = 1$ **(f)** $\alpha = 1$, $\beta = 1$

Figure 4. Graphical representation of $Re[u_1^{\pm}(x,t)]$.

The real sections of the $Re[u_5^{\pm}(x,t)]$ for $3D$ and $2D$ graphs $b = 1$, $p = 1$, $v = 2$, $k_2 = 1$, $o = 1$, $h = 0.1$, $k_1 = 3$, $a_1 = 5$, $a_2 = 2$, $g = -1$ are shown in Figure 5 by assigning various parameter values. The legend in Figure 5 indicates the line graphs of $Re[u_5^{\pm}(x,t)]$ for $t = 1$, $t = 2$, and $t = 3$. Figure 5 presents profiles of periodic waves.

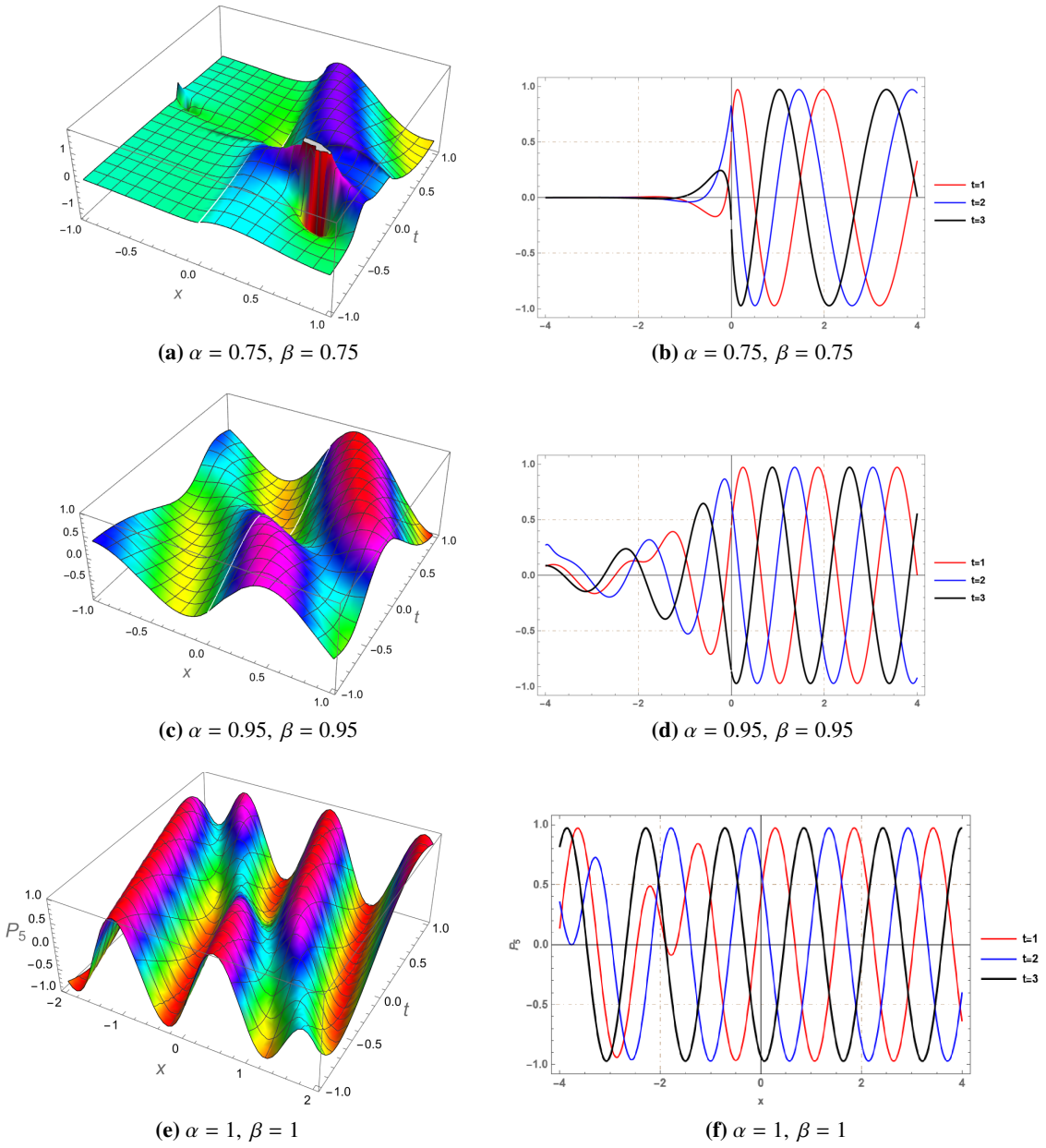

(a) $\alpha = 0.75$, $\beta = 0.75$ **(b)** $\alpha = 0.75$, $\beta = 0.75$

(c) $\alpha = 0.95$, $\beta = 0.95$ **(d)** $\alpha = 0.95$, $\beta = 0.95$

(e) $\alpha = 1$, $\beta = 1$ **(f)** $\alpha = 1$, $\beta = 1$

Figure 5. Graphical representation of $Re[u_5^{\pm}(x,t)]$.

8. Conclusions

In this study, we employed the Hamiltonian formulation, the Ritz methodology, the variational approach based on the variational principle, and the modified Sardar subequation method to obtain traveling wave solutions of nonlinear fractional Schrödinger equations. A comparison with the results already reported in literature is also shown in Table 1. The governing equations were transformed into nonlinear ordinary differential equations through a fractional complex transformation. These methods proved effective and reliable for constructing precise analytical wave solutions, including bright, dark, singular, and periodic solitons. The resultant wave structures provide about the dynamical behavior. The findings reported here are novel and advance our undestanding of fractional wave propagation,

particularly the role of conformable fractional derivatives. The diversity of solutions obtained suggests potential applications in communication technology and optical fiber design. This work presents a broader class of solutions and underscores the usefulness of fractional effects in optical systems, in contrast to previous research that primarily focused on the mEDAM approach. Furthermore, these results pave the way for future extensions and numerical investigations in more intricate physical environments.

Table 1. Advantages of selected analytical and variational methods over other available methods.

Method	Key advantages	Advantage over other methods
Modified Sardar Sub-equation	Closed-form solutions; exhibits novel solution families.	Gives precise solutions, more comprehensive than other analytical techniques.
He's Semi-Inverse Method	Formulates Lagrangians;offers semi-analytical or analytical solutions; reduces problem complexity	constructs the functional methodically and does not require a prior functional; gives analytical solutions unlike numerical methods.
Ritz Method	Efficient; controllable accuracy via trial functions; suitable for BVPs and complex geometries	More flexible than exact analytical methods; more efficient than purely numerical approaches.
Hamiltonian-Based Approach	Conserves energy/momentum; offers qualitative dynamics; useful for integrability and soliton solutions	Preserves intrinsic conserved quantities; valuable for stability and long-term evolution analysis.

Author contributions

Tahani A. Alrebdi, Nauman Raza, Saima Arshed, F. Alkallas and Abdel-Haleem Abdel-Aty: Conceptualization, Methodology, Software, Validation, Writing-original draft, Writing-review and editing. All authors of this article have contributed equally. All authors read and approved the final manuscript.

Use of Generative-AI tools declaration

The authors declare they have not used Artificial Intelligence (AI) tools in the creation of this article.

Acknowledgments

The authors extend their appreciation to the Deanship of Scientific Research and Libraries in Princess Nourah bint Abdulrahman University for funding this research work through the Research Group project, Grant No. (RG-1445-0044).

Conflict of interest

No conflicting interests are disclosed by the authors.

References

1. S. Saifullah, N. Fatima, S. Abdelmohsen, M. Alanazi, S. Ahmad, D. Baleanu, Analysis of a conformable generalized geophysical KdV equation with Coriolis effect, *Alex. Eng. J.*, **73** (2023), 651–663. https://doi.org/10.1016/j.aej.2023.04.058
2. C. Qiao, X. Long, L. Yang, Y. Zhu, W. Cai, Calculation of a dynamical substitute for the real Earth-Moon system based on Hamiltonian analysis, *ApJ*, **991** (2025), 46. https://doi.org/10.3847/1538-4357/adf73a
3. P. Li, R. Gao, C. Xu, Y. Li, A. Akgül, D. Baleanu, Dynamics exploration for a fractional-order delayed zooplankton phytoplankton system, *Chaos Soliton. Fract.*, **166** (2023), 112975. https://doi.org/10.1016/j.chaos.2022.112975
4. C. Xu, E. Balci, Hunting cooperation and gestation delay in a prey-predator model with fractional derivative, *J. Appl. Anal. Comput.*, **16** (2026), 1035–1053. https://doi.org/10.11948/20250147
5. W. Sun, Y. Jin, G. Lu, Y. Liu, Stabilizer testing and central limit theorem, *Phys. Rev. A*, **111** (2025), 32421. https://doi.org/10.1103/PhysRevA.111.032421
6. A. Kumar, H. Chauhan, C. Ravichandran, K. Nisar, D. Baleanu, Existence of solutions of non-autonomous fractional differential equations with integral impulse condition, *Adv. Differ. Equ.*, **2020** (2020), 434. https://doi.org/10.1186/s13662-020-02888-3
7. A. Freihet, S. Hasan, M. Al-Smadi, M. Gaith, S. Momani, Construction of fractional power series solutions to fractional stiff system using residual functions algorithm, *Adv. Differ. Equ.*, **2019** (2019), 95. https://doi.org/10.1186/s13662-019-2042-3
8. N. Laskin, Fractional Schrödinger equation, *Phys. Rev. E*, **66** (2002), 056108. https://doi.org/10.1103/PhysRevE.66.056108
9. N. Laskin, Fractional quantum mechanics and Lévy path integrals, *Phys. Lett. A*, **268** (2000), 298–305. https://doi.org/10.1016/S0375-9601(00)00201-2
10. N. Raza, M. Rafiq, A. Bekir, H. Rezazadeh, Optical solitons related to (2+1)-dimensional Kundu-Mukherjee-Naskar model using an innovative integration architecture, *J. Nonlinear Opt. Phys.*, **31** (2022), 2250014. https://doi.org/10.1142/S021886352250014X
11. M. Naber, Time fractional Schrödinger equation, *J. Math. Phys.*, **45** (2004), 3339–3352. https://doi.org/10.1063/1.1769611
12. B. Guo, Y. Han, J. Xin, Existence of the global smooth solution to the period boundary value problem of fractional nonlinear Schrödinger equation, *Appl. Math. Comput.*, **204** (2008), 468–477. https://doi.org/10.1016/j.amc.2008.07.003
13. D. Yang, Z. Du, Asymptotic analysis of double-hump solitons for a coupled fourth-order nonlinear Schrödingier system in a birefringent optical fiber, *Chaos Soliton. Fract.*, **199** (2025), 116831. https://doi.org/10.1016/j.chaos.2025.116831

14. R. Eid, S. Muslih, D. Baleanu, E. Rabei, On fractional Schrödinger equation in α-dimensional fractional space, *Nonlinear Anal.-Real*, **10** (2009), 1299–1304. https://doi.org/10.1016/j.nonrwa.2008.01.007

15. S. Muslih, O. Agrawal, D. Baleanu, A fractional Schrödinger equation and its solution, *Int. J. Theor. Phys.*, **49** (2010), 1746–1752. https://doi.org/10.1007/s10773-010-0354-x

16. J. Gomez-Aguilar, D. Baleanu, Schrödinger equation involving fractional operators with non-singular kernel, *J. Electromagnet. Wave.*, **31** (2017), 752–761. https://doi.org/10.1080/09205071.2017.1312556

17. T. Bakkyaraj, R. Sahadevan, Approximate analytical solution of two coupled time fractional nonlinear Schrödinger equations, *Int. J. Appl. Comput. Math.*, **2** (2016), 113–135. https://doi.org/10.1007/s40819-015-0049-3

18. S. Longhi, Fractional Schrödinger equation in optics, *Opt. Lett.*, **40** (2015), 1117–1120. https://doi.org/10.1364/OL.40.001117

19. G. P. Agrawal, Nonlinear fiber optics: its history and recent progress, *J. Opt. Soc. Am. B*, **22** (2011), A1–A10. https://doi.org/10.1364/JOSAB.28.0000A1

20. B. Malomed, Multidimensional solitons: well-established results and novel findings, *Eur. Phys. J. Spec. Top.*, **225** (2016), 2507–2532. https://doi.org/10.1140/epjst/e2016-60025-y

21. C. Xu, M. Ur Rahman, H. Emadifar, Bifurcations, chaotic behavior, sensitivity analysis and soliton solutions of the extended Kadometsevâ-Petviashvili equation, *Opt. Quant. Electron.*, **56** (2024), 405. https://doi.org/10.1007/s11082-023-05958-4

22. J. He, Variational principles for some nonlinear partial differential equations with variable coefficients, *Chaos Soliton. Fract.*, **19** (2004), 847–851. https://doi.org/10.1016/S0960-0779(03)00265-0

23. M. Murad, H. Ismael, T. Sulaiman, Various exact solutions to the time-fractional nonlinear Schrödinger equation via the new modified Sardar sub-equation method, *Phys. Scr.*, **99** (2024), 085252. https://doi.org/10.1088/1402-4896/ad62a6

24. M. Alabedalhadi, Exact travelling wave solutions for nonlinear system of spatiotemporal fractional quantum mechanics equations, *Alex. Eng. J.*, **61** (2022), 1033–1044. https://doi.org/10.1016/j.aej.2021.07.019

25. Q. Wang, Homotopy perturbation method for fractional KdV-Burgers equation, *Chaos Soliton. Fract.*, **35** (2008), 843–850. https://doi.org/10.1016/j.chaos.2006.05.074

26. Y. Tian, J. Liu, A modified exp-function method for fractional partial differential equations, *Therm. Sci.*, **25** (2021), 1237–1241. https://doi.org/10.2298/TSCI200428017T

27. M. Bayrak, A. Demir, A new approach for space-time fractional partial differential equations by residual power series method, *Appl. Math. Comput.*, **336** (2018), 215–230. https://doi.org/10.1016/j.amc.2018.04.032

28. A. Esen, F. Bulut, Ö. Oruç, A unified approach for the numerical solution of time fractional Burgersâ type equations, *Eur. Phys. J. Plus*, **131** (2016), 116. https://doi.org/10.1140/epjp/i2016-16116-5

29. O. Abu Arqub, Numerical simulation of time-fractional partial differential equations arising in fluid flows via reproducing Kernel method, *Int. J. Numer. Method. H.*, **30** (2020), 4711–4733. https://doi.org/10.1108/HFF-10-2017-0394

30. M. Eslami, B. Fathi Vajargah, M. Mirzazadeh, A. Biswas, Application of first integral method to fractional partial differential equations, *Indian J. Phys.*, **88** (2014), 177–184. https://doi.org/10.1007/s12648-013-0401-6

31. A. Gaber, H. Ahmad, Solitary wave solutions for space-time fractional coupled integrable dispersionless system via generalized kudryashov method, *FU-Math. Inform.*, **35** (2020), 1439–1449. https://doi.org/10.22190/FUMI2005439G

32. R. Shah, H. Khan, P. Kumam, M. Arif, D. Baleanu, Natural transform decomposition method for solving fractional-order partial differential equations with proportional delay, *Mathematics*, **7** (2019), 532. https://doi.org/10.3390/math7060532

33. M. Sarıkaya, H. Budak, H. Usta, On generalized the conformable fractional calculus, *TWMS J. Appl. Eng. Math.*, **9** (2019), 792–799.

AIMS Press